J Appl Physiol 105: 711–717, 2008.
First published May 1, 2008; doi:10.1152/japplphysiol.00949.2007.

Unrestrained acoustic plethysmograph for measuring specific airway resistance in mice

Jeffrey S. Reynolds,[1] Victor J. Johnson,[2] and David G. Frazer[1]

[1]*Pathology and Physiology Research Branch and* [2]*Toxicology and Molecular Biology Research Branch, Health Effects Laboratory Division, National Institute for Occupational Safety and Health, Morgantown, West Virginia*

Submitted 6 September 2007; accepted in final form 25 April 2008

Reynolds JS, Johnson VJ, Frazer DG. Unrestrained acoustic plethysmograph for measuring specific airway resistance in mice. *J Appl Physiol* 105: 711–717, 2008. First published May 1, 2008; doi:10.1152/japplphysiol.00949.2007.—An acoustic whole body plethysmograph was developed to estimate specific airway resistance (sRaw) in unrestrained mice. The plethysmograph uses acoustic principles to measure the thoracic breathing pattern and simultaneously measures the airflow entering and/or leaving the plethysmograph. Similarly to traditional methods utilizing a double-chamber plethysmograph, these measurements were combined to estimate sRaw. To evaluate the new system, we placed six conscious A/J mice individually in a whole body plethysmograph (Buxco System) for a 2-min exposure to aerosolized methacholine chloride dissolved in saline (0, 5, 10, and 20 mg/ml), which is known to increase sRaw in mice. Three minutes after exposure, the mice were transferred to the acoustic plethysmograph for 2 min for data collection. The mean baseline value of sRaw was 0.93 ± 0.10 $cmH_2O \cdot s$. A dose-dependent increase in sRaw was shown, with an approximate tripling of sRaw at the highest dose. These results demonstrate the ability of the system to estimate sRaw based on plethysmograph airflow and acoustic amplitude.

Helmholtz resonator; unrestrained plethysmograph; whole body plethysmograph

TRADITIONALLY, THE DOUBLE-CHAMBER PLETHYSMOGRAPH has been used to estimate specific airway resistance (sRaw) (15) from the phase shift between flows measured at the thorax and at the nasal passage. In recent years, there has been a growing interest in measuring sRaw using the unrestrained (or single chamber) whole body plethysmograph (WBP). This type of plethysmograph is easy to use, allows repeated measurements in the same subject, and produces little stress in the animal. The disadvantage is that the single available pressure measurement is influenced by the mechanical properties of the airways and the shape of the breathing pattern. Isolating the component related to airway resistance is difficult, perhaps impossible, without a second measurement.

The most popular parameter derived using the single-chamber plethysmograph is an empirical index called Penh (9) that was said to reflect changes in airway reactivity. However, a number of articles have questioned the relationship between Penh and the mechanical properties of the lung (1, 3, 6, 14, 18, 22). Recently, other parameters have been developed that relate more closely to lung mechanics. Lundblad et al. (13) showed that the pressure measured in the unrestrained plethysmograph could be written as a function of airway resistance, functional residual capacity, and tidal volume when the chamber air is conditioned to body temperature and humidity. Lai-Fook and Lai (10) developed an estimate of airway resistance based on the area under the plethysmograph pressure curve, functional residual capacity, and tidal volume. As both these groups have pointed out, these methods may reflect changes in resistance, although it is necessary to either assume that the thoracic breathing pattern is not altered during or between measurements or obtain some measure of the thoracic breathing pattern. Such a system for obtaining this extra measure was recently reported by Bates et al. (2), who described an unrestrained video plethysmograph.

Similarly, we present a novel acoustic whole body plethysmograph (AWBP) capable of measuring sRaw. The plethysmograph not only acts as a traditional WBP but also uses acoustic principles to measure the thoracic breathing pattern (19). sRaw is then based on the phase shift between these two measurements, much like methods utilizing the double-chamber plethysmograph.

MATERIALS AND METHODS

System

This system is a modification of the previously described plethysmograph (19), which uses acoustics to measure the thoracic breathing pattern. Briefly, the plethysmograph operates as a resonating cavity. The amplitude of the acoustic pressure inside the cavity is determined by the cavity geometry. The volume of air surrounding a respiring mouse changes by the change in size of the mouse as it breathes. When the system is excited near the resonant frequency, the acoustic pressure amplitude in the plethysmograph is modulated in direct proportion to the change in volume of the mouse.

In the previously described system (19), a low-resistance nozzle was used to maximize the sensitivity of the system to changes in mouse volume. In that system, the nozzle resistance was too low to use as a pneumotachograph to measure the traditional WBP box flow. The current implementation is shown in Fig. 1. The speaker produces a constant-frequency (~300 Hz) acoustic signal. The micrometer is used to adjust the volume surrounding the mouse so that the chamber is in a near resonant condition and changes in mouse volume produce linear changes in the acoustic pressure amplitude (see Ref. 19). A screen placed across the outside end of the plethysmograph nozzle acts as a pneumotachograph to enable measurement of box flow. The pressure drop across the screen was measured with a differential pressure transducer (Setra Systems, model 239). So the modified plethysmograph provides two measurements. A signal proportional to change in mouse volume is measured with a microphone from the high-frequency (relative to breathing frequency), low-amplitude (acoustic) pressure changes. The traditional WBP signal is measured

Address for reprint requests and other correspondence: J. S. Reynolds, Pathology and Physiology Research Branch, Health Effects Laboratory Division, National Institute for Occupational Safety and Health, 1095 Willowdale Rd., ms L2101, Morgantown, WV 26505 (e-mail: jsr0@cdc.gov).

The costs of publication of this article were defrayed in part by the payment of page charges. The article must therefore be hereby marked "*advertisement*" in accordance with 18 U.S.C. Section 1734 solely to indicate this fact.

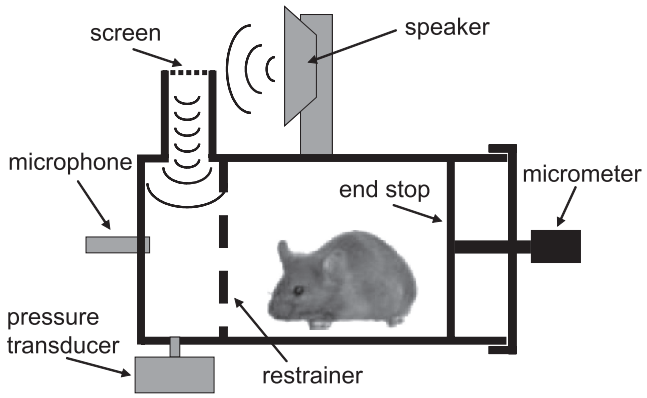

Fig. 1. Schematic of the modified acoustic plethysmograph. The speaker generates a constant frequency (~300 Hz) that resonates the air in the chamber. The micrometer is used to adjust the chamber volume. Movement of the animal chest wall modulates the sound amplitude, which is measured by the microphone. The pressure transducer measures the pressure drop across the screen, which is proportional to flow into and out of the chamber. The restrainer inhibits the animal from occluding the nozzle.

from the low-frequency change in plethysmograph pressure, which is proportional to box flow. The restrainer keeps the mouse from occluding the nozzle, which would affect both measurements.

Although the acoustic plethysmograph is designed to be a second-order system having a resonant frequency near 300 Hz, Sinnett et al. (21) have shown that these types of flow plethysmographs act as first-order systems at low frequencies. Furthermore, they have shown that a flow plethysmograph with a first-order time constant of 1.5 ms or less has a fast enough response for accurate measurement of forced vital capacity maneuvers in mice. Given the AWBP volume (~75 ml) and screen resistance (0.00224 $cmH_2O \cdot s \cdot ml^{-1}$), the first-order time constant is ~0.168 ms in isothermal conditions and 0.120 ms in adiabatic conditions. Since we are inferring flow from pressure at low frequencies (mouse breathing frequencies, <10 Hz), whether the system operates in either an adiabatic or isothermal mode (or changes between the two) has little effect on the box flow measurement.

Model

sRaw is derived from a model (15) of the respiratory system as shown in Fig. 2*A*. The current source, I_t, represents the thoracic flow produced by the animal. Z_t represents the impedance of the lung tissues, I_a represents flow in the airways, R_a represents the flow resistance of the airways, and C_g represents the compressibility of the gas in the lung and airways. P_t and P_{ao} represent the pressures (relative to atmospheric pressure) produced at the thorax and airway opening, respectively. P_{alv} is alveolar pressure, and P_{atm} is atmospheric pressure. Note that the direction of the currents indicated in Fig. 2 are for expiration and are reversed during inspiration.

When an animal respires air at room conditions, the gas is warmed and humidified on inspiration, and the reverse (approximately) takes place on expiration. Therefore, there is an effective change in volume flow due to this thermohygrometric effect. This thermohygrometric "flow" (I_{th}) is in phase with I_a and can be modeled as

$$I_{th} = GI_a \quad (1)$$

where G (5) is given as

$$G = \left[1 - \frac{T_c(P_a - P_{H_2O_a})}{T_a(P_c - P_{H_2O_c})}\right] \quad (2)$$

where the subscripts c and a denote conditions of chamber and alveolar gas, respectively, and T and P are absolute temperature and pressure, respectively. Incorporating this effect results in the model shown in Fig. 2*B*.

It has been suggested that differences between inspiratory and expiratory conditions would necessitate separate calculations of G (7, 12, 14). Consider an animal placed inside a WBP. During inspiration, the gas is warmed from chamber temperature to body temperature and

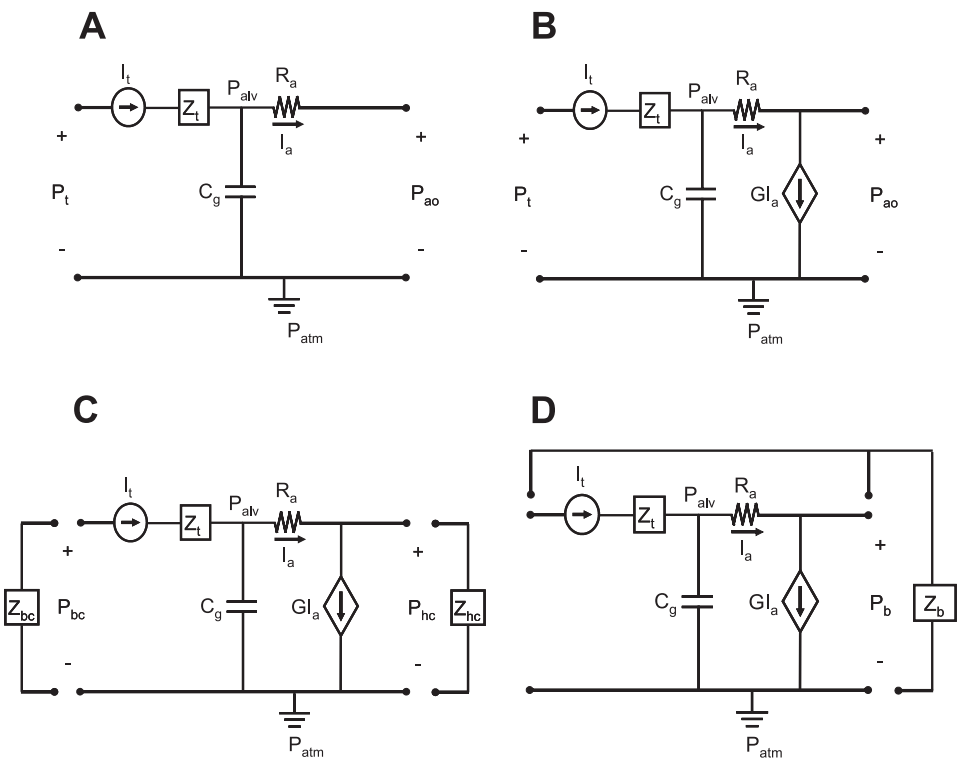

Fig. 2. Development of the whole body plethysmograph electric circuit analog model. *A*: simple model of the respiratory system (15). I_t represents flow produced by the thorax, Z_t represents tissue impedance, R_a is airway resistance, and C_g represents compliance of alveolar gas. P_t represents pressure produced at the thorax, and P_{ao} is pressure at the airway opening. P_{alv} and P_{atm} represent alveolar and atmospheric pressure, respectively. *B*: the term GI_a represents the flow "lost" on expiration ("gained" on inspiration) due to changes in temperature and humidity. *C*: model of the animal placed in a restrained, or double-chamber, plethysmograph. Z_{bc} and Z_{hc} represent the flow impedances of the body chamber and head chamber, respectively. P_{bc} and P_{hc} are the pressures measured in the body chamber and head chamber, respectively. *D*: model of the animal placed in an unrestrained, or whole body plethysmograph. Z_b represents the box flow impedance, and P_b represents the box pressure.

humidified from chamber humidity to saturation. In humans, expiratory gas exits at nasal conditions of ~32°C and saturated with water vapor (7). Whereas the human respiratory tract is not a very efficient heat exchanger, that of the small rodent is much more efficient. Schmid (20) studied the exit temperature of respired air for many small mammals, including several species of mouse, and found the exit temperature to be ~1°C above ambient.

Consider a mouse inspiring air at 50% relative humidity and 22°C, with expiratory conditions of 100% relative humidity and 23°C. For this case, the inspiratory value of G is 0.0956 and the expiratory value is 0.0816, a difference of ~17%. For an animal placed in a chamber with an open nozzle, the relative humidity in the chamber will increase with each breath until the moisture added per breath is equal to the moisture leaving the chamber via diffusion. Therefore, the inspiratory G will move toward the expiratory G the longer the animal stays in the chamber, so there is a slight variation in G from inspiration to expiration during tidal breathing. Also, small baseline changes in G might occur if the efficiency of heating and cooling is affected by changes in respiratory rate, depth of breathing, and core temperature, among others. The model used in this research considers a fixed G estimated as the average of the inspiratory G calculated at room conditions and the expiratory G calculated at 100% relative humidity and 1°C above room temperature. Room temperature and relative humidity during this research were 22.7°C and 47%, respectively. Using an assumed body temperature of 37°C resulted in an average G of 0.084.

Now consider an animal placed in a double-chamber plethysmograph (DCP), which is the traditional system used to estimate sRaw. This system uses a neck seal to enable simultaneous measurement of nasal flow and thoracic flow. Figure 2*C* shows the electric circuit analog corresponding to the DCP. Z_{bc} represents the impedance of the body chamber, and Z_{hc} represents the impedance of the head chamber. This system restrains the animal but allows independent measurements of two flows (or pressures) from which sRaw can be estimated.

When an animal is placed in an unrestrained WBP, there is an interaction between the thorax and nasal flows (i.e., no neck seal). Figure 2*D* shows the electric circuit analog corresponding to the WBP. In this case, Z_b represents the box impedance. Without modification, this circuit can be redrawn as shown in Fig. 3. This represents the low-frequency bulk flow model of the WBP.

Mathematical description. An expression for sRaw can be derived based on the model shown in Fig. 3. Summing the currents in the lung,

$$I_a(t) + I_c(t) - I_t(t) = 0 \tag{3}$$

where $I_c(t)$ is the current into the capacitor, C_g, such that

$$I_c(t) = C_g \frac{dP_{alv}(t)}{dt} \tag{4}$$

Alveolar pressure is

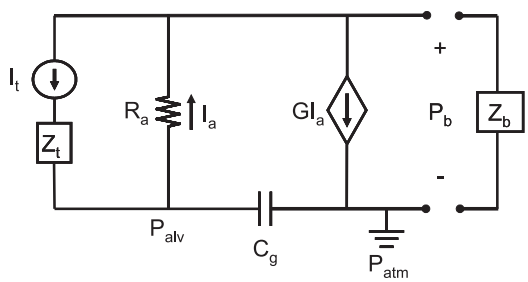

Fig. 3. Model of animal in the unrestrained plethysmograph. This model is exactly the same circuit as in Fig. 2*D*. It has been redrawn in a more concise manner.

$$P_{alv}(t) = R_a I_a(t) + P_b(t) \approx R_a I_a \tag{5}$$

Since the box pressure, P_b, is extremely small compared with alveolar pressure, the box pressure term can be neglected. Substituting into the preceding equation gives

$$I_c(t) = R_a C_g \frac{dI_a(t)}{dt} \tag{6}$$

Now substituting this expression into *Eq. 3* and solving for thoracic flow gives

$$I_t(t) = I_a(t) + R_a C_g \frac{dI_a(t)}{dt} \tag{7}$$

Summing the currents at the airway opening,

$$I_b(t) + I_a(t) - GI_a(t) - I_t(t) = 0 \tag{8}$$

Solving for airway flow gives

$$I_a(t) = \frac{I_t(t) - I_b(t)}{1 - G} \tag{9}$$

Substituting into *Eq. 7* and rearranging gives

$$I_b(t) + R_a C_g \frac{dI_b(t)}{dt} = GI_t(t) + R_a C_g \frac{dI_t(t)}{dt} \tag{10}$$

Taking the Laplace transform,

$$I_b(s) + R_a C_g I_b(s)s = GI_t(s) + R_a C_g I_t(s)s \tag{11}$$

$$I_b(s)(1 + R_a C_g s) = I_t(s)(G + R_a C_g s) \tag{12}$$

The transfer function from thoracic flow to box flow, I_b, is

$$\frac{I_b(s)}{I_t(s)} = \frac{G + R_a C_g s}{1 + R_a C_g s} \tag{13}$$

The transfer function from thoracic volume, V_t, to box volume, V_b, is then equal to the transfer function from thoracic flow to box flow:

$$\frac{I_b(s)}{I_t(s)} = \frac{s \cdot V_b(s)}{s \cdot V_t(s)} = \frac{V_b(s)}{V_t(s)} = \frac{G + R_a C_g s}{1 + R_a C_g s} \tag{14}$$

Since the derivative is inherently noisy, it is more convenient to integrate box flow and use volume signals than to take the derivative of thoracic volume and use flow signals. Substituting $s = j\omega$:

$$\frac{V_b(j\omega)}{V_t(j\omega)} = \frac{G + j\omega R_a C_g}{1 + j\omega R_a C_g} \tag{15}$$

$$\frac{V_b(j\omega)}{V_t(j\omega)} = \frac{G + j\omega R_a C_g}{1 + j\omega R_a C_g} \cdot \frac{1 - j\omega R_a C_g}{1 - j\omega R_a C_g} \tag{16}$$

$$\frac{V_b(j\omega)}{V_t(j\omega)} = \frac{G + \omega^2 R_a^2 C_g^2 + j(1 - G)\omega R_a C_g}{1 + \omega^2 R_a^2 C_g^2} \tag{17}$$

so the phase angle, θ, between thoracic volume and box volume is given as

$$\tan\theta = \frac{(1 - G)\omega R_a C_g}{G + \omega^2 R_a^2 C_g^2} \tag{18}$$

Rearranging gives

$$\omega^2 \tan\theta (R_a C_g)^2 - \omega(1 - G) R_a C_g + G \tan\theta = 0 \tag{19}$$

Solving for $R_a C_g$,

$$R_aC_g = \frac{(1 - G) \pm \sqrt{(1 - G)^2 - 4G\tan^2\theta}}{2\omega\tan\theta} \quad (20)$$

Only the smaller root of the *Eq. 20* yields physiologically relevant values (see Appendix):

$$R_aC_g = \frac{(1 - G) - \sqrt{(1 - G)^2 - 4G\tan^2\theta}}{2\omega\tan\theta} \quad (21)$$

Alternately, dropping the higher order term of *Eq. 19* provides reasonable accuracy. This results in the following solution:

$$R_aC_g = \frac{G\tan\theta}{2\pi(1 - G)f} \quad (22)$$

Where frequency, f, is $f = \omega/(2\pi)$. Results presented in this research were calculated using *Eq. 21*.

Specific airway resistance. Specific airway resistance is defined as

$$\text{sRaw} = R_a \cdot \text{TGV} \quad (23)$$

where TGV is thoracic gas volume. Gas compliance in the lung (assuming isothermal conditions) can be written as

$$C_g = \frac{\text{TGV}}{P_{atm} - P_{H_2O_a}} \quad (24)$$

By substitution of *Eq. 24* into *Eq. 23*, it is seen that sRaw is the time constant R_aC_g multiplied by pressure $P_{atm} - P_{H_2O_a}$:

$$\text{sRaw} \equiv R_a \cdot C_g \cdot [P_{atm} - P_{H_2O_a}] \quad (25)$$

In this research, the measurements were made over a relatively short span of time. Therefore, the pressure term can be considered a constant, and R_aC_g is then a direct measure of sRaw. In this study, estimates of R_aC_g have units given in milliseconds. However, if sRaw is estimated based on $P_{atm} - P_{H_2O_a} \approx 1{,}000$ cmH_2O, then from *Eq. 25*,

$$\text{sRaw} = R_aC_g \text{ ms} \cdot 1{,}000 \text{ cm}H_2O \quad (26)$$

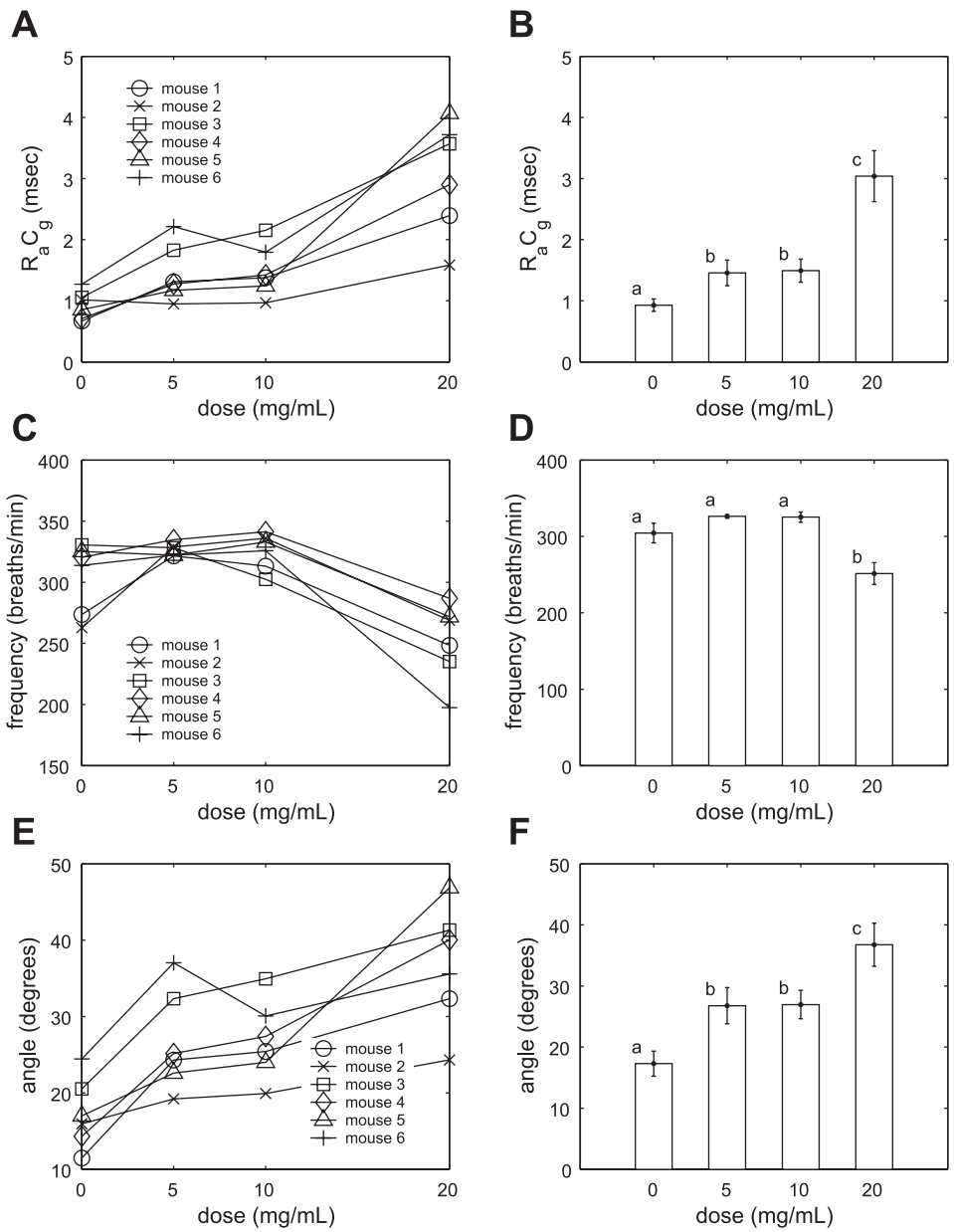

Fig. 4. Results (means ± SE) of the methacholine aerosol exposure. *A*: individual R_aC_g dose responses. *B*: average R_aC_g dose response. *C*: individual phase-shift dose responses. *D*: average phase-shift dose response. *E*: individual breathing frequency dose responses. *F*: average breathing frequency dose response. [a,b,c]Lowercase letters denote statistically significant differences.

$$= 1{,}000 \cdot R_a C_g \text{ cmH}_2\text{O}\cdot\text{ms} \quad (27)$$

$$= R_a C_g \text{ cmH}_2\text{O}\cdot\text{s} \quad (28)$$

Under these conditions, sRaw in units of $\text{cmH}_2\text{O}\cdot\text{s}$ will have the same numerical value as R_aC_g in units of milliseconds.

Experimental design. Six 21.0 (SD 1.7)-g, specific pathogen-free female A/J mice (Jackson Laboratory) were housed in an American Association for Accreditation of Laboratory Animal Care-accredited animal facility at 23°C and 50% humidity with a 12:12-h light-dark cycle and were provided standard laboratory mouse chow and tap water ad libitum. Each mouse was placed in a chamber for a 2-min exposure to aerosolized methacholine chloride dissolved in saline (0, 5, 10, and 20 mg/ml). Three minutes after exposure, the mice were transferred to the acoustic plethysmograph for 2 min, where box flow and thoracic volume were measured at a sampling rate of 2,000 Hz. Since all six mice were tested at each concentration before increase to the next concentration of methacholine, the time between doses for each mouse was ~45 min. All animal procedures were performed following an animal protocol approved by the National Institute for Occupational Safety and Health Institutional Animal Care and Use Committee.

Statistics. All experimental data (means ± SE) were analyzed using one-way ANOVA followed by post hoc analysis using Fisher's protected least significant difference. Log transformation was applied to equalize variance between doses. Dose-response trends were determined using regression analysis. Differences were considered significant at $P < 0.05$.

Signal Processing

The electromechanical delay between the pressure transducer and the microphone was assessed by lightly tapping the nozzle opening with no animal in the chamber. This produced a pressure drop across the screen while simultaneously interrupting the acoustic signal measured by the microphone. These data were used to calculate the phase shift produced by the electromechanical properties of the transducers, which was subsequently subtracted from the phase shift measured with the animal present in the plethysmograph.

The animal data were processed as follows. A 15-Hz low-pass filter was applied to the data for noise reduction. Box flow was integrated to obtain box volume. The data were broken into 6-s segments with a 50% overlap; that is, the first segment is from $t = 0$ s to $t = 6$ s, the second segment from $t = 3$ s to $t = 9$ s, and so on. An estimate of the transfer function was computed using Welch's averaged periodogram method (Matlab "tfe" function) with a 4,000-point transform size, a 4,000-point window, and an overlap of 2,000 samples. By using these same parameters, an estimate of the coherence was determined for each segment.

For each segment, the angle of the transfer function was determined at the breathing frequency by linear interpolation from the estimate above. This angle and breathing frequency were used with *Eq. 21* to calculate an estimate of R_aC_g for each segment. Similarly, coherence for each segment was determined at the breathing frequency. The mean R_aC_g value was found by averaging the estimates for all the segments whose coherence was ≥0.9.

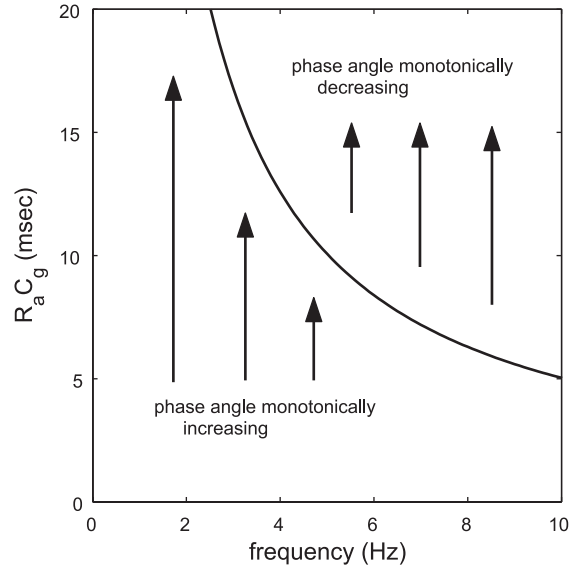

Fig. 6. For any given frequency, the model phase shift increases monotonically with R_aC_g up to a maximum phase (denoted by the line), after which the phase angle decreases.

RESULT

The results of the methacholine aerosol exposure are shown in Fig. 4. At doses of 5 and 10 mg/ml, five of the six mice had

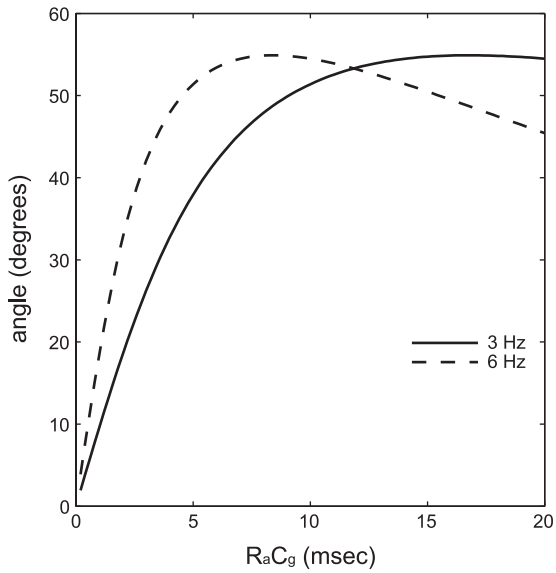

Fig. 5. Curves represent the theoretical phase response, as a function of R_aC_g, of the model for 2 different frequencies.

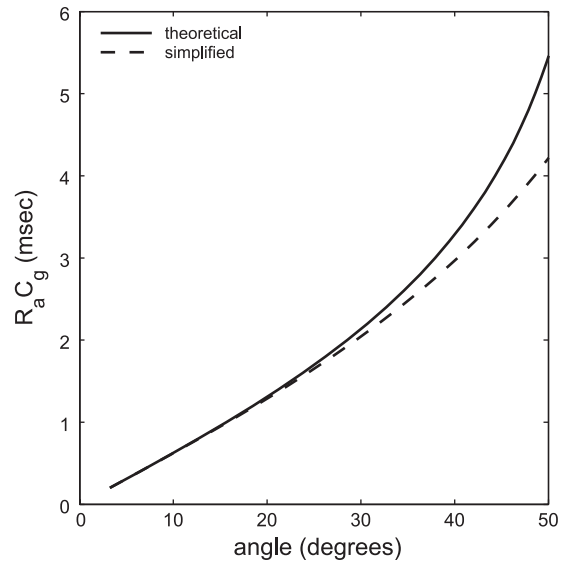

Fig. 7. R_aC_g as predicted from the model phase shift at a frequency of 5 Hz. The solid line represents the exact solution (*Eq. 21*). The dashed line represents the solution to the simplified expression (*Eq. 22*).

elevated R_aC_g compared with baseline (Fig. 4*A*). At the highest methacholine dose (20 mg/ml), each mouse had an increased R_aC_g compared with saline. The mean R_aC_g dose-response curve is shown in Fig. 4*B*. The mean increase from baseline for doses of 5 and 10 mg/ml was 57 and 61%, respectively. At the 20 mg/ml dose, the mean increase was >227%, or a little more than a tripling of R_aC_g.

The airway resistance-compliance values were calculated based on the phase shift and the breathing frequency. The results for these two component measurements are shown in Fig. 4, *C–F*. In general, there was a dose-dependent increase in phase shift accompanied by a decrease in breathing frequency at the highest dose.

DISCUSSION

The signal measured from a spontaneously respiring animal in the traditional WBP is generated from the thoracic flow of the animal, filtered by the mechanical properties of the airways. Therefore, changes in this signal can result from either changes in the thoracic flow pattern or changes in the respiratory "filter." The drawback of past methods utilizing the unrestrained plethysmograph is that to relate changes in the filter (i.e., sRaw) based solely on changes in the WBP signal, it must be assumed that the thoracic flow pattern is unchanged. The plethysmograph presented in this research overcame this issue by allowing measurement of the thoracic flow signal in addition to the WBP signal. This allows assessment of R_aC_g even in cases where the breathing pattern of the animal is significantly affected.

The baseline sRaw value of 0.93 ± 0.10 $cmH_2O \cdot s$ obtained in this research is consistent with previously reported baseline values in A/J mice. Lofgren et al. (11) found a baseline sRaw value of 0.676 ± 0.027 $cmH_2O \cdot s$ in A/J mice using a restrained WBP. However, in a direct comparison of systems using BALB/c mice, they found that sRaw determined in their restrained WBP was about one-third the value they measured using a DCP. Delorme and Moss (4) measured sRaw in A/J mice using a DCP. In two trials performed a minimum of 2 days apart, they found values of 1.68 ± 0.06 and 1.49 ± 0.14 $cmH_2O \cdot s$. In addition, our baseline results are nearly identical to those of Flandre et al. (8) for BALB/c and C57BL/6 mice, measured using a DCP.

Direct comparison of dose-response curves is inexact, since the actual delivered dose is affected by the specific nebulizer, airflow, tubing arrangement, and such. However, there is general agreement in our results and those of Lofgren et al. (11), particularly at the highest dose used, where sRaw was elevated and the breathing frequency was depressed.

The modified acoustic plethysmograph does present some technical difficulties that can be addressed in future revisions. The addition of a screen to the plethysmograph nozzle adds significant acoustic resistance to the system. This in turn reduces volume sensitivity. This reduction in sensitivity complicates calibration of the volume signal and allows significant noise degradation of the volume measurement. On the other hand, a higher screen resistance increases the sensitivity and noise immunity of box pressure measurements. The ideal solution (and future improvement) would be a device for measuring nozzle flow that has little flow resistance.

Although a low-resistance flowmeter would be ideal, the method presented in this research allows us to overcome the shortcomings of measuring flow with a screen pneumotach. We have presented a method of estimating R_aC_g that is dependent only on the phase of the transfer function. As described in the Appendix, using only phase does limit the range of measurable R_aC_g. The ability to use magnitude and phase information over a range of frequencies is desirable and would likely remove these limitations. However, the limits of R_aC_g using phase are high enough that they are likely irrelevant for assessing the pulmonary response of the mouse in most cases. Because we are only using phase, it is not necessary to calibrate the thoracic volume or the box volume signal, since the magnitude is unimportant. Furthermore, even in the presence of significant noise on the thoracic volume signal, we are able to measure the increase in sRaw due to methacholine exposure using only the phase information.

Although the results are preliminary in nature, we have described a modified acoustic plethysmograph that allows measurement of both the traditional unrestrained plethysmograph flow signal and the thoracic volume signal in mice. Furthermore, a method of using the phase shift between these signals to evaluate R_aC_g has been provided. This system provides an efficient and accurate method of assessing specific airway resistance of mice in an unrestrained plethysmograph.

APPENDIX

To infer sRaw from the phase shift of the transfer function given in *Eq. 17*, *Eq. 19* must be solved for R_aC_g. Since *Eq. 19* is quadratic in R_aC_g, the phase angle, θ, initially increases with an increase in R_aC_g but eventually reaches a peak and then decreases as R_aC_g continues to increase. As a result, there are two solutions for any given phase shift. Figure 5 displays the phase angle vs. airway resistance-compliance for the model at two frequencies and $G = 0.1$. A reasonable approach is to use only the portion of the curve that is monotonically increasing (that is, the smaller of the 2 solutions).

It can be shown that the value of the peak angle is constant for a constant G. However, the phase angle reaches a peak at a lower R_aC_g as frequency increases. The curve denoting the peak angle (which is constant for constant G) as a function of frequency and R_aC_g is shown in Fig. 6. Given the breathing frequency f, this curve defines the maximum R_aC_g that can be inferred from the phase angle. As an example, consider a mouse breathing at 5 Hz. As the animal's airways constrict, the phase angle would increase until R_aC_g reaches ~10 ms. As the airways continue to narrow, the phase would begin to drop, appearing as though R_aC_g were actually decreasing. However, since the R_aC_g for normal mice is ~1 ms, it would appear to be an extreme case for R_aC_g to cross the limit shown in Fig. 6. Even for a mouse breathing at the unusually high frequency of 10 Hz, airway resistance-compliance could quintuple before the limit would be reached.

Finally, for $f = 5$ Hz, Fig. 7 displays R_aC_g as a function of the phase angle for *Eqs. 21* and *22*. The simplified expression of *Eq. 22* produces a slight underestimation of R_aC_g. For assessing mice whose R_aC_g is in the range of normal to 300% of normal, *Eq. 22* provides reasonable accuracy.

DISCLOSURES

The findings and conclusions of this report are those of the authors and do not necessarily represent the views of the National Institute for Occupational Safety and Health.

REFERENCES

1. **Adler A, Cieslewicz G, Irvin CG.** Unrestrained plethysmography is an unreliable measure of airway responsiveness in BALB/c and C57BL/6 mice. *J Appl Physiol* 97: 286–292, 2004.
2. **Bates JHT, Thompson-Figueroa J, Lundblad LKA, Irvin CG.** Unrestrained video-assisted plethysmography: a noninvasive method for assessment of lung mechanical function in small animals. *J Appl Physiol* 104: 253–261, 2008.
3. **Drazen JM, Finn PW, De Sanctis GT.** Mouse models of airway responsiveness: physiological basis of observed outcomes and analysis of selected examples using these outcome indicators. *Annu Rev Physiol* 61: 593–625, 1999.
4. **DeLorme MP, Moss OR.** Pulmonary function assessment by whole-body plethysmography in restrained versus unrestrained mice. *J Pharmacol Toxicol Methods* 47: 1–10, 2002.
5. **Drorbaugh JE, Fenn WO.** A barometric method for measuring ventilation in newborn infants. *Pediatrics* 16: 81–87, 1955.
6. **Enhorning G, van Schaik S, Lundgren C, Vargas I.** Whole-body plethysmography, does it measure tidal volume in small animals? *Can J Physiol Pharmacol* 76: 945–951, 1989.
7. **Epstein MAF, Epstein RA.** A theoretical analysis of the barometric method for measurement of tidal volume. *Respir Physiol* 32: 105–120, 1978.
8. **Flandre TD, Leroy PL, Desmecht DJM.** Effect of somatic growth, strain, and sex on double-chamber plethysmographic respiratory function values in healthy mice. *J Appl Physiol* 94: 1129–1136, 2003.
9. **Hamelmann E, Schwarze J, Takeda K, Oshiba A, Larsen GL, Irvin CG, Gelfand EW.** Noninvasive measurement of airway responsiveness in allergic mice using barometric plethysmography. *Am J Respir Crit Care Med* 156: 766–775, 1997.
10. **Lai-Fook SJ, Lai Y.** Airway resistance due to alveolar gas compression measured by barometric plethysmography in mice. *J Appl Physiol* 98: 2204–2218, 2005.
11. **Lofgren LS, Mazan MR, Ingenito EP, Lascola K, Seavey M, Walsh A, Hoffman AM.** Restrained whole body plethysmography for measure of strain-specific and allergen induced airway responsiveness in conscious mice. *J Appl Physiol* 101: 1495–1505, 2006.
12. **Lomask M.** Further exploration of the Penh parameter. *Exp Toxicol Pathol* 57, *Suppl* 2: 13–20, 2006.
13. **Lundblad LKA, Irvin CG, Adler A, Bates JHT.** A reevaluation of the validity of unrestrained plethysmography in mice. *J Appl Physiol* 93: 1198–1207, 2002.
14. **Mitzner W, Tankersley C, Lundblad LKA, Irvin CG, Adler A, Bates JHT.** A reevaluation of the validity of unrestrained plethysmography in mice. *J Appl Physiol* 94: 828–832, 2003.
15. **Pennock BE, Cox CP, Rogers RM, Cain WA, Wells JH.** A noninvasive technique for measurement of changes in specific airway resistance. *J Appl Physiol* 46: 399–406, 1979.
16. **Peslin R, Duvivier C, Vassiliou M, Gallina C.** Thermal artifacts in plethysmographic airway resistance measurements. *J Appl Physiol* 79: 1958–1965, 1995.
17. **Peslin R, Duvivier C.** Removal of thermal artifact in alveolar pressure measurement during forced oscillation. *Respir Physiol* 117: 141–150, 1999.
18. **Petak F, Habre W, Danati YR, Hantos Z, Barazzone-Argiroffo C.** Hyperoxia-induced changes in mouse lung mechanics: forced oscillations vs barometric plethysmography. *J Appl Physiol* 90: 2221–2230, 2001.
19. **Reynolds JS, Frazer DG.** Unrestrained acoustic plethysmograph for measuring tidal volume in mice. *Ann Biomed Eng* 34: 1494–1499, 2006.
20. **Schmid WD.** Temperature gradients in the nasal passage of some small mammals. *Comp Biochem Physiol* 54A: 304–308, 1975.
21. **Sinnett EE, Jackson AC, Leith DE, Butler JP.** Fast integrated flow plethysmograph for small mammals. *J Appl Physiol* 50: 1104–1110, 1981.
22. **Sly PD, Turner DJ, Collins RA, Hantos Z.** Penh is not a validated technique for measuring airway function in mice. *Am J Respir Crit Care Med* 172: 256, 2005.